Protection of telomeres by a conserved Stn1–Ten1 complex

Victoria Martín*†, Li-Lin Du*‡, Sophie Rozenzhak*, and Paul Russell*§¶

Departments of *Molecular Biology and §Cell Biology, The Scripps Research Institute, La Jolla, CA 92037

Communicated by Donald R. Helinski, University of California at San Diego, La Jolla, CA, June 25, 2007 (received for review February 22, 2007)

Telomeres are specialized chromatin structures that protect chromosome ends. Critical among telomere proteins are those that bind the telomeric single-strand DNA (ssDNA) overhangs. These proteins are thought to differ among eukaryotes. Three interacting proteins (Cdc13, Stn1, and Ten1) associate with the telomeric overhang in budding yeast, a single protein known as Pot1 (protection of telomeres-1) performs this function in fission yeast, and a two-subunit complex consisting of POT1 and TPP1 associates with telomeric ssDNA in humans. Cdc13 and Pot1 have related oligonucleotide/oligosaccharide-binding fold (OB-fold) domains that bind the telomeric ssDNA overhang. Here we show that *Schizosaccharomyces pombe* has Stn1- and Ten1-like proteins that are essential for chromosome end protection. Stn1 orthologs exist in all species that have Pot1, whereas Ten1-like proteins can be found in all fungi. Fission yeast Stn1 and Ten1 localize at telomeres in a manner that correlates with the length of the ssDNA overhang, suggesting that they specifically associate with the telomeric ssDNA. Unlike in budding yeast, in which Cdc13, Stn1, and Ten1 all interact, fission yeast Stn1 and Ten1 associate with each other, but not with Pot1. Our findings suggest that two separate protein complexes are required for chromosome end protection in fission yeast. Structural profiling studies detect OB-fold domains in Stn1 and Ten1 orthologs, indicating that protection of telomeres by multiple proteins with OB-fold domains is conserved in eukaryotic evolution.

fission yeast | oligonucleotide/oligosaccharide-binding fold | POT1
Schizosaccharomyces pombe

Preservation of genome integrity in eukaryotic organisms depends on telomeres, which are specialized chromatin structures that compose the ends of linear chromosomes (1, 2). Telomeres cap and protect chromosome ends, shielding them from the DNA repair and cell cycle checkpoint machinery. Failure to properly protect chromosome ends leads to chromosome end-to-end fusions and other genome rearrangements, further leading to forms of genomic instability typically associated with cancer. Telomeres are also essential for recruiting telomerase, the enzyme that adds telomeric DNA to the 3′ ends of chromosomes.

In most species, telomeric DNA consists of short tandem repeats terminating in a 3′ G-rich single-stranded DNA (ssDNA) overhang (1, 2). This overhang is recognized by telomeric ssDNA-binding proteins, of which *Oxytricha nova* telomere end-binding protein (TEBP) is the prototype. Other well studied end-binding proteins are Cdc13, which is from the budding yeast *Saccharomyces cerevisiae*, and Pot1, which is conserved in the fission yeast *Schizosaccharomyces pombe*, humans, and other diverse species. Loss of Cdc13 in budding yeast leads to resection of the C-rich telomeric strand, activation of the DNA damage checkpoint, and subsequent cell death (3–6). A similar response is seen in fission yeast *pot1*Δ mutants, although *pot1*Δ survivors can arise by circularization of their three chromosomes through end-to-end fusions (7).

Structural data on Cdc13, Pot1, and TEBP have shown that recognition of telomeric ssDNA occurs through a conserved motif, the oligonucleotide/oligosaccharide-binding fold (OB-fold) domain. The OB-fold domain is a compact structural motif of bacterial origin found in a variety of proteins that interact with ssDNA. In addition to Pot1 and Cdc13, OB-fold domain-containing proteins include the three subunits of replication protein A (RPA) (Fig. 1*A*), several types of DNA helicases and ligases, and the breast cancer susceptibility gene 2 (BRCA2) protein (8, 9). Superposition of the OB-folds in TEBPα and the initially described OB-fold of *S. cerevisiae* Cdc13 and *S. pombe* Pot1 indicates that the central core of the domain is conserved, although the outer regions of the OB-fold are more variable (10–13). Human POT1 has two OB-folds in its DNA-binding domain. Moreover, the human POT1-interacting protein, TPP1, has been recently identified as the human homolog of TEBPβ based on the structure of its OB-fold domain (14, 15). This observation, together with the recent identification of tandem OB-folds in Cdc13 and Pot1 (16), suggests that recognition of telomeric ssDNA through multiple OB-folds may be a conserved feature of telomere-capping proteins.

The structural commonalities of their OB-folds suggest that Cdc13 and Pot1 are related. However, the weak sequence similarity of the OB-folds, the absence of sequence similarity outside of these domains, and their different domain organizations (Fig. 1*A*) have left uncertain whether Pot1 and Cdc13 are orthologous proteins (10). Cdc13 associates with two other proteins, Stn1 and Ten1, which are essential for telomere protection (1, 17–20). A recent study showed that Stn1 and Ten1 are ssDNA-binding proteins that bind with enhanced specificity to telomeric DNA sequences, leading to the idea that a Cdc13–Stn1–Ten1 complex functions as an RPA-like complex that is specific for telomeres (21).

Here we report the discovery of two proteins that colocalize with Pot1 on the telomeric overhangs in fission yeast. These proteins, which are essential for chromosome end protection, are distantly related to budding yeast Stn1 and Ten1.

Results

Identification of *S. pombe* SPBC409.12C as an OB-Fold-Containing Protein Related to Stn1. The prevalence of OB-fold domains in proteins involved in DNA replication, repair, and recombination processes led us to search for OB-fold domain-encoding sequences in the fission yeast genome database. One predicted ORF highlighted by this bioinformatics approach was the orphan gene SPBC409.12C, which was listed as encoding a 229-aa protein with a partial OB-fold motif at its extreme N terminus (Fig. 1*B*). The presence of a partial OB-fold motif suggested that SPBC409.12C might be incorrectly annotated. Indeed, analysis of mRNAs by 5′

Author contributions: V.M., L.-L.D., and P.R. designed research; V.M., L.-L.D., and S.R. performed research; V.M., L.-L.D., and P.R. analyzed data; and V.M. and P.R. wrote the paper.

The authors declare no conflict of interest.

Abbreviations: CFP, cyan fluorescent protein; OB-fold, oligonucleotide/oligosaccharide-binding fold; PFGE, pulsed-field gel electrophoresis; RPA, replication protein A; TEBP, telomere end-binding protein.

†Present address: Department of Molecular Biology, University of Geneva, Sciences III, CH-1211 Geneva, Switzerland.

‡Present address: National Institute of Biological Sciences, Beijing 102206, China.

¶To whom correspondence should be addressed. E-mail: prussell@scripps.edu.

This article contains supporting information online at www.pnas.org/cgi/content/full/0705497104/DC1.

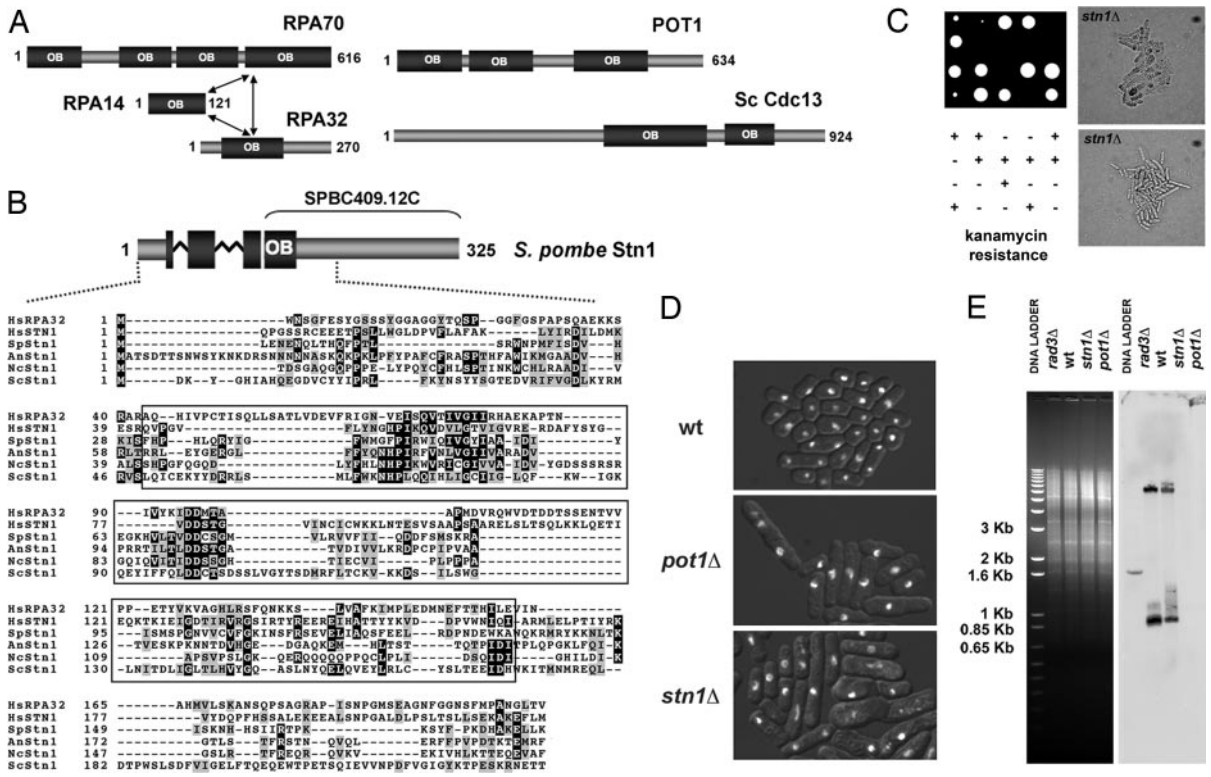

Fig. 1. Stn1 homologs and analysis of fission yeast *stn1*Δ cells. (*A*) Schematic showing the human RPA, human POT1, and budding yeast Cdc13 OB-fold domain structure. The model for the structural organization of the RPA trimer was previously described (23). The positions of the multiple OB-fold domains in POT1 and Cdc13 are based on previously published data (16). (*B*) (*Upper*) Schematic representation of *S. pombe* Stn1. The protein fragment previously annotated as SPBC409.12C is shown. The N-terminal OB-fold of Stn1 is represented as a fragmented box to show the partial OB-fold present in SPBC409.12C and the one obtained by adding the N-terminal sequences obtained during our 5′ RACE analyses. Zig-zag lines indicate the position of the two introns in the 5′ region of the corresponding gene. (*Lower*) Multiple alignment of the N-terminal regions of the Stn1 orthologs in Hs, *Homo sapiens* (NP_079204); Sp, *S. pombe* (CAB52614); An, *Aspergillus nidulans* (XP_663844); Nc, *Neurospora crassa* (XP_960343); and Sc, *S. cerevisiae* (CAA98902). Alignment of human RPA32 is also provided. Residues included in the predicted OB-fold domains of the different proteins appear boxed. PSI-BLAST indicates that the sequence similarities of the OB-fold domains are highly significant [e.g., SpStn1 (3–129) vs. HsStn1 (11–158), *E* value = $2e^{-40}$; SpStn1 (19–160) vs. HsRPA32 (47–182), *E* value = $4e^{-21}$]. (*C*) Tetrad dissection of the heterozygous *stn1*Δ diploid strain (*Left*), and cell morphology of the *stn1*Δ haploid null mutants (*Right*). Two colonies at the ≈20-cell stage were photographed. (*D*) Fluorescence images of DNA stained with Hoechst 33342 were overlaid on bright-field images of the cells. Cells came from colonies formed after spores were incubated at 30°C for 3 days. The mutant colonies contained ≤2,000 cells. The mutants displayed similar phenotypes. A significant number of mutant cells are elongated or misshapen. Hoechst staining showed unevenly divided DNA in many mutant cells. (*E*) Loss of TAS1 telomeric-proximal DNA in *stn1*Δ cells. EcoRI-digested genomic DNA was subjected to electrophoresis and stained with ethidium bromide (*Left*) before its transfer to a membrane and hybridization to a TAS1 probe (*Right*). Genomic DNA from wild-type (wt), *rad3*Δ, and *pot1*Δ strains was used as controls.

RACE and nested PCR showed that transcripts spanning SPBC409.12C contain two 5′-proximal introns that, when spliced out, yield an mRNA that encodes a 325-aa protein [Fig. 1*B* and supporting information (SI) Fig. 5]. Structural profiling of this protein was performed by using the 3D position-specific scoring matrix (3D-PSSM) program (22). The analysis predicted the presence of a complete OB-fold domain in the N-terminal region of full-length SPBC409.12C. This OB-fold domain is most similar to that in the N terminus of human RPA32 (*E* value = 0.222; >80% confident prediction). Interestingly, this domain is one of the contact sites for ssDNA in RPA (23).

Position-specific iterated BLAST (PSI-BLAST) showed that SPBC409.12C belongs to a family of proteins conserved in a broad range of eukaryotes (Fig. 1*B*) (24, 25). The human homolog is a 368-aa protein annotated as OB-fold-containing 1 (OBFC1). According to 3D-PSSM, OBFC1 has an N-terminal OB-fold domain that also is most similar to that in human RPA32 (*E* value = 0.0747; >90% confident prediction) (Fig. 1*B*). PSI-BLAST confirmed the sequence relationships of SPBC409.12C, OBFC1, and RPA32 (Fig. 1*B*), indicating that they share a common ancestor.

Additional PSI-BLAST iterations revealed that *S. cerevisiae* Stn1 is a highly diverged member of the SPBC409.12C/OBFC1 protein family (Fig. 1*B*). 3D-PSSM indicated that the N-terminal region of Stn1 also might have an OB-fold domain similar to that in RPA32 (*E* value = 6.96). Stn1 is essential for telomere end protection in budding yeast (20). Its apparent absence in other species has fueled speculation that telomere-capping mechanisms are fundamentally different between budding yeast and most other eukaryotes. The identification of potential Stn1 orthologs in humans and fission yeast, and the fact that they have OB-fold motifs, was therefore of considerable interest.

Stn1 Is Essential for Telomere Maintenance in Fission Yeast. To date, the only known single-strand telomere-specific binding protein in fission yeast is Pot1 (7). If SPBC409.12C is an Stn1 ortholog and it is essential for telomere protection, an SPBC409.12C knockout should be identical to *pot1*Δ. Side-by-side tetrad analyses of heterozygous SPBC409.12C or *pot1*$^+$ knockout diploids were performed to test this prediction. As seen for the *pot1*Δ, the SPBC409.12C knockout (*stn1*Δ) spores were initially only able to form microcolonies that were invisible to the naked eye, whereas the wild-type spores from the same tetrads produced fast-growing colonies. Microscopic analyses of the microcolonies (≈20–40 cells) on the agar plate showed that they consisted mostly of elongated and/or misshapen cells, the majority of which appeared to be dead (Fig. 1*C*). At the ≈2,000-cell stage, a substantial number of the

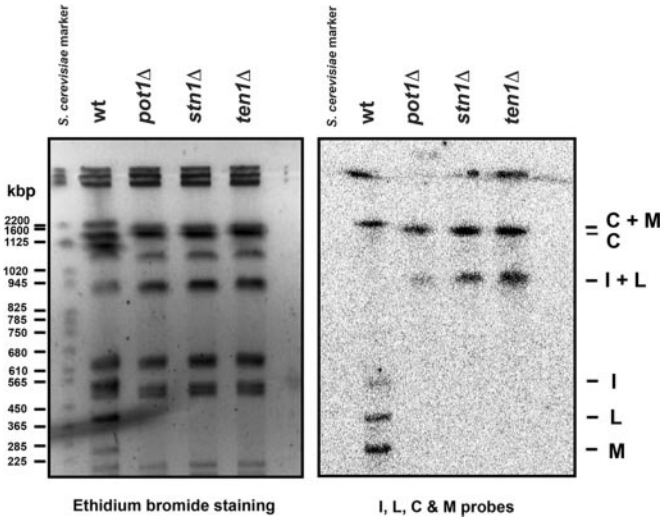

Fig. 2. NotI-digested *S. pombe* chromosomal DNAs from the indicated haploid strains were fractionated in 1% agarose gel with 0.5× TBE buffer at 14°C by using a CHEF-DR II system (Bio-Rad, Hercules, CA) at 200 V and a pulse time of 60–120 sec for 30 h. The marker lane contained *S. cerevisiae* chromosomal DNA (Bio-Rad). Ethidium bromide-stained PFGE gel (*Left*) and hybridization of the same gel with probes specific for *S. pombe* telomere proximal NotI fragments C, M, I, and L (*Right*) are shown. In the mutant strains, these fragments are absent and have been replaced by DNA fragments C+M and I+L.

SPBC409.12C knockout cells remained elongated and/or misshapen. Hoechst 33342 staining showed unevenly divided DNA in many of these cells (Fig. 1*D*). A subset of cells appeared similar to wild type, and, upon longer incubation, a relatively healthy population of these cells emerged to the extent that it was difficult to differentiate between wild-type cells and SPBC409.12C knockouts. This pattern of phenotypes was identical to that of the *pot1*Δ cells that we analyzed and those described by Baumann and Cech (7), who showed that the healthy *pot1*Δ survivors arise through end-to-end fusions leading to chromosome circularization. Indeed, *stn1*Δ *pot1*Δ double mutants were created by tetrad dissection and found to be identical to the single mutants (data not shown).

To specifically address whether SPBC409.12C is required for telomere maintenance, Southern analyses were performed to detect telomeric-associated sequences (TAS1) in wild-type cells and the SPBC409.12C knockout (*stn1*Δ) and *pot1*Δ survivors. This experiment showed that TAS1 DNA was absent in *stn1*Δ and *pot1*Δ cells (Fig. 1*E*), something reported only in *S. pombe pot1* mutants, which survive complete telomere loss through intrachromosomal end fusions (26).

To test whether *stn1*Δ cells survived the loss of the terminal part of their chromosomes by circularizing their chromosomes, we performed pulsed-field gel electrophoresis (PFGE) analysis of NotI-digested genomic DNAs. As shown in Fig. 2, PFGE and Southern hybridization analysis confirmed that *stn1*Δ survivors had lost I and L telomeric fragments and gained a fragment of the size expected of an I+L fusion resulting from the circularization of chromosome I. This pattern was identical to that seen in the *pot1*Δ survivors. This experiment also indicated a C+M fusion involving circularization of chromosome II in the *stn1*Δ and *pot1*Δ survivors, although this analysis was complicated by the apparently anomalous C fragment in the wild-type control used in this experiment. From these results, we conclude that SPBC409.12C is a true Stn1 ortholog, and its function is essential to maintain telomeres.

A Ten1-Like Protein Protects Fission Yeast Telomeres. In *S. cerevisiae*, Stn1 and Cdc13 associate with Ten1, a 160-aa protein that is

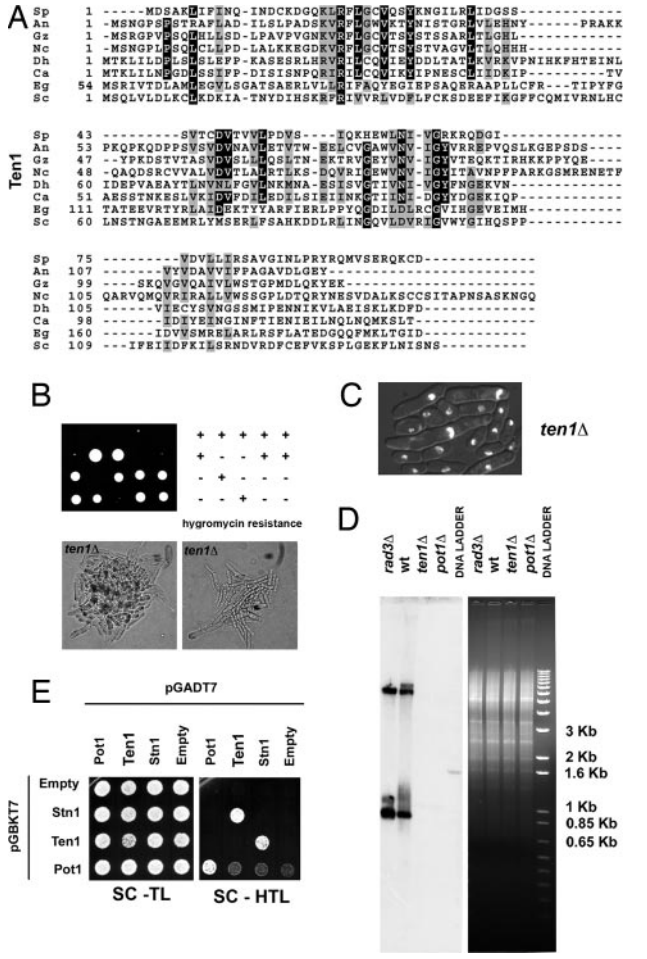

Fig. 3. Ten1 homologs and analysis of fission yeast *ten1*Δ cells. (*A*) Alignment of Ten1 proteins from *S. pombe* and other different fungi. Sp, *Schizosaccharomyces pombe* (see main text for sequence information); An, *A. nidulans* (unannotated ORF, nucleotides 229341–229625 of FGSC A4 chromosome 2); Nc, *N. crassa* (CAE76110); Dh, *Debaryomyces hansenii* (XP_462449); Sc, *S. cerevisiae*; Gz, *Gibberella zeae* (unannotated ORF, nucleotides 9551–9826 of NRRL 31084 chromosome 1); Ca, *Candida albicans* (XP_717945); Eg, *Eremothecium gossypii* (NP_984444). (*B–D*) Analysis of *ten1*Δ equivalent to Fig. 1 *C–E*. (*E*) Yeast two-hybrid analysis showing the self-interaction of fission yeast Pot1–Pot1 and the Stn1–Ten1 interactions.

essential for telomere end protection (19). Previous bioinformatic studies failed to identify conserved motifs in Ten1 or uncover homologs in *S. pombe* and several other yeast species. The discovery of an Stn1 ortholog in fission yeast prompted us to carry out a new search for Ten1-like proteins in fission yeast. PSI-BLAST and motif searching highlighted an ORF spanning the 25586–25278 region of cosmid SPCC1393, which was not annotated as a gene in the *S. pombe* databases (SI Fig. 6). The sequence of the predicted 102-aa protein is only weakly similar to budding yeast Ten1. However, sequence alignments reveal that it is a member of an uncharacterized family of distantly related proteins found in highly divergent fungal species, including *Neurospora crassa*, *Gibberalla zeae*, and *Aspergillus nidulans* (Fig. 3*A* and SI Fig. 7). Related proteins were not found in nonfungal species, perhaps because they have diverged beyond recognition by sequence-alignment tools. Interestingly, 3D-PSSM analyses indicated that the putative Ten1 homologs have an OB-fold domain that is most closely related to that found in the anticodon-binding domain of aspartyl-tRNA synthetases (e.g., *N. crassa*, *E* value = 0.384; *G. zeae*, *E* value = 0.934; *A. nidulans*, *E* value = 1.93; SI Fig. 8).

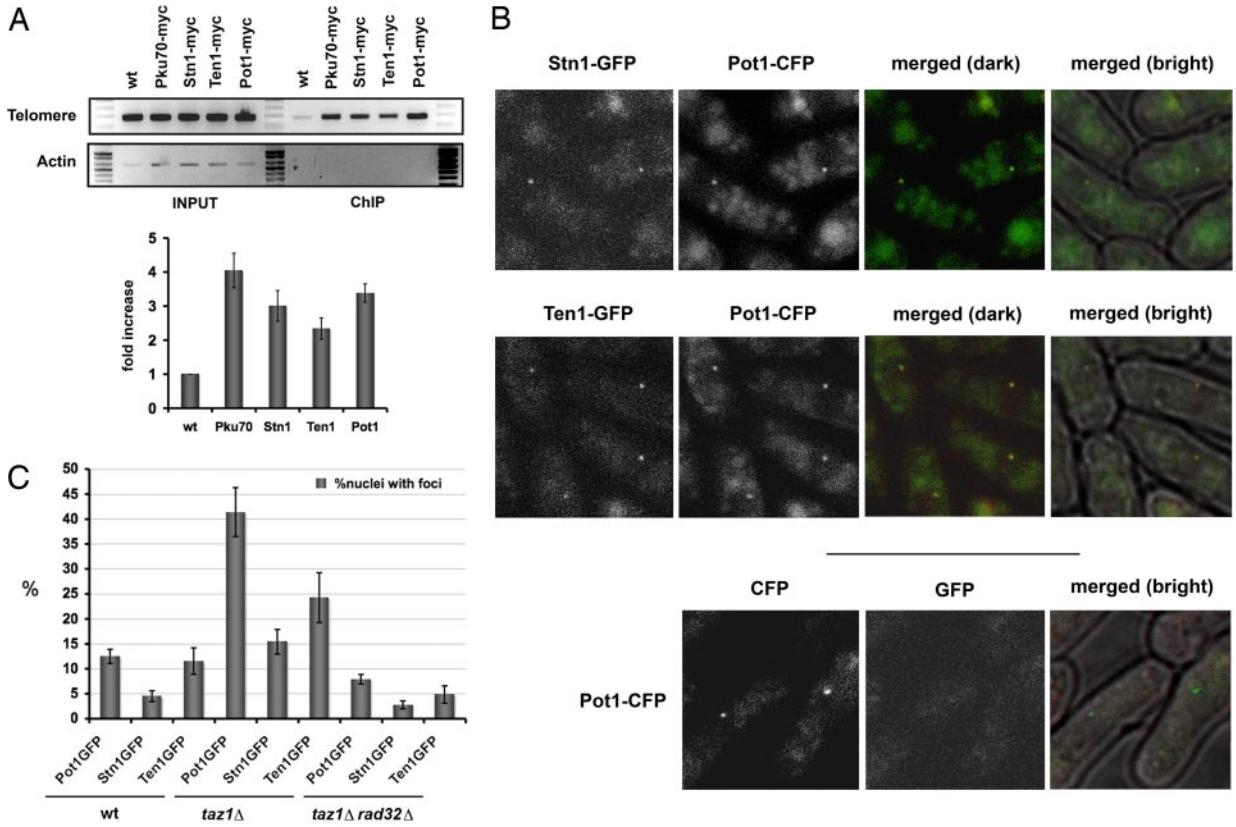

Fig. 4. *S. pombe* Ten1, Stn1, and Pot1 proteins colocalize and bind to telomeres. (*A*) ChIP assays measuring the association of myc-tagged Stn1, Ten1, Pot1, and Pku70 with TAS1 relative to the *act1*$^+$ genomic region. Samples were normalized to an untagged wild-type (wt) control. Error bars indicate standard deviations derived from three independent experiments. (*B*) Fluorescence microscopy of endogenously GFP-tagged Stn1 and Ten1 in live cells. GFP and cyan fluorescent protein (CFP) signals from strain VM365 (*taz1*Δ, *pot1–CFP*, *stn1–GFP*) (*Top*) and VM364 (*taz1*Δ, *pot1–CFP*, *ten1–GFP*) (*Middle*) were analyzed. Overlays of fluorescence images (merged dark) or overlays of fluorescence images with bright-field (merged bright) images showed that Ten1–GFP and Stn1–GFP nuclear foci colocalize with Pot1–CFP in the *taz1*Δ background. Images of cells expressing Pot1-CFP alone showed that no bleedthrough occurred between the CFP and GFP channels (*Bottom*). Similarly, no CFP signal was detected in strains that expressed only Stn1–GFP or Ten1–GFP (data not shown). The diffuse cytoplasmic signal is a background fluorescence signal observed in untagged controls. (*C*) Foci formation of Pot1–GFP, Stn1–GFP, and Ten1–GFP analyzed in wild-type, *taz1*Δ, and *taz1*Δ *rad32*Δ backgrounds. Quantification of the percentage of nuclei-containing foci is shown. At least 200 cells were analyzed for each of the strains. Error bars indicate standard deviations.

Tetrad dissections showed that spores having a knockout mutation in the putative *ten1* ortholog have the same phenotypes as *stn1*Δ and *pot1*Δ spores (Fig. 3 *B* and *C*). Southern and PFGE analyses confirmed that the *ten1*Δ survivors lost TAS1 in a manner consistent with chromosome circularization (Figs. 2 and 3*D*). From these observations, we conclude that the predicted 102-aa protein identified as a Ten1-like protein is indeed a Ten1 ortholog that is required for chromosome end protection.

Stn1 and Ten1 Colocalize with Pot1 at Telomeres. Because budding yeast Cdc13, Stn1, and Ten1 were initially reported to interact in yeast two-hybrid assays (17, 19, 20), we performed the same analyses with fission yeast Pot1, Stn1, and Ten1. These analyses revealed Stn1–Ten1 and Pot1–Pot1 interactions, but Pot1 failed to interact with Stn1 or Ten1 (Fig. 3*E*). These data suggest that an Stn1–Ten1 heterodimeric complex functions without associating with a Pot1–Pot1 homodimeric complex. Precedent for such a mechanism comes from *O. nova* TEBP, whose α and β subunits can form two alternative complexes, an α–α homodimer and an α–β heterodimer that bind specifically but differently to telomeric overhangs (27). Alternatively, the two complexes may associate to form a larger complex only upon binding to telomeric ssDNA. Such a mechanism would not be unprecedented. Taking *O. nova* TEBP as a model again, its α- and β-subunits exist predominantly as monomers *in vitro* but form a stable complex in the presence of telomeric ssDNA (27). Because it is unknown to what extent Cdc13, Ten1, and Stn1 form a stable complex, it is possible that binding telomeric ssDNA stabilizes the interactions among these three proteins.

ChIP studies have shown that Cdc13 localizes at telomeres (28). Recombinant *S. cerevisiae* Stn1 and Ten1 proteins bind telomeric single-stranded substrates *in vitro*, which suggests that they bind telomeres *in vivo* (21). We performed ChIP assays to determine whether Pot1, Stn1, and Ten1 localize at telomeres in fission yeast. These assays were performed with strains in which the endogenous loci encoded myc-tagged proteins. The cell growth and morphology of the tagged strains were indistinguishable from the wild-type cells, which indicated that the fusion proteins were functional. The precipitated chromatin fragments were amplified by PCR with primers specific for the TAS1 and the *act1*$^+$ gene from fission yeast. Pku70-myc served as a positive control (Fig. 4*A*), confirming earlier studies performed in our laboratory (26). Our results showed specific interactions of Pot1, Stn1, and Ten1 with TAS1 but not with *act1*$^+$ (Fig. 4*A*). No such enrichment was observed when using an untagged strain, indicating that the binding of Pku70, Pot1, Stn1, and Ten1 to telomeres is specific.

We attempted to confirm these results in colocalization experiments using fluorescent protein-tagged versions of Pot1, Stn1, and Ten1 expressed from their genomic loci. As seen with the myc-tagged strains, these strains had normal growth rates and morphology, indicating that the fluorescent protein-tagged versions of Pot1, Stn1, and Ten1 were functional. For each protein, we detected faint

nuclear foci in ≈5–15% of live cells (data not shown). We were able to demonstrate that the Pot1 foci colocalized with the telomere-binding protein Taz1 (data not shown). However, the Stn1 and Ten1 signals were too weak for the colocalization assay, perhaps indicating that the concentration of Stn1 and Ten1 at chromosome ends is lower than that of Pot1. This observation is in agreement with our yeast two-hybrid data and ChIP results, which suggest that the Stn1–Ten1 heterodimer and Pot1 might not bind chromosome ends as a stable complex.

Based on the hypothesis that Stn1 and Ten1 should be binding ssDNA, we decided to carry on our colocalization studies in a different strain background, in which recruitment of both proteins to the telomere ssDNA overhangs could be favored. The telomere-binding protein Taz1 is a fission yeast ortholog of mammalian TRF1 and TRF2 proteins (29). Taz1 acts as a negative regulator of telomere length. In *taz1*Δ cells, telomere length and length heterogeneity are dramatically increased, and there is an intense telomeric G-strand ssDNA overhang signal (29–31). We reasoned that if Stn1 and Ten1 are recruited to telomeric ssDNA overhangs, the amounts of Stn1 and Ten1 localized at telomeres of *taz1*Δ cells would increase concomitant with an increase in Pot1, which was in fact the case. Because the signals were stronger, we could show that Stn1–GFP and Ten1–GFP colocalized in foci with Pot1–cyan fluorescent protein (CFP) (Fig. 4*B*). In other studies, we found that Pot1, Stn1, and Ten1 do not form foci in response to ionizing radiation (data not shown), and thus their colocalization in *taz1*Δ cells cannot be explained by a model in which they recognize telomeres in *taz1*Δ cells as sites of DNA damage. Our results show that Stn1 and Ten1 colocalize with Pot1 at telomeres, but the relative strength of GFP and CFP signals suggests that the abundance of Pot1 at telomeres is greater than that of Stn1 or Ten1. In human cells, ChIP studies have shown that longer telomeres contain more Pot1, which suggests that Pot1 may associate with other telomeric proteins that are bound to double-stranded repeat arrays (32). A similar situation is conceivable in fission yeast.

It is thought that Cdc13 and Pot1 associate with the telomeric overhang *in vivo*. As mentioned earlier, telomere elongation in *taz1*Δ mutants is accompanied by an increase in the G-strand overhang. We wanted to determine whether the increased binding of Pot1, Stn1, and Ten1 to telomeres in *taz1*Δ mutants correlates with the increased ssDNA overhang. Telomere elongation in *taz1*Δ mutants does not require the $Mre11^{Rad32}$ subunit of the Mre11–Rad50–Nbs1 DNA repair complex, but $Mre11^{Rad32}$ is required for the appearance of the G-strand overhang (30). We therefore examined the localization of endogenously GFP-tagged versions of Pot1, Stn1, and Ten1 in the *taz1*Δ *rad32*Δ cells. In these cells, the percentage of nuclei containing foci of any of the three proteins was strongly decreased to well below the amounts seen in wild-type cells (Fig. 4*C*). From these results, we conclude that the residence of Pot1, Stn1, and Ten1 at telomeres is largely, if not completely, dependent on the presence of telomeric ssDNA.

Discussion

The critical role of the telomere end protection family of proteins is to shield the 3′ single-stranded telomere overhang from degradation and misrecognition as broken DNA. The crystal structures of TEBP, Cdc13, and Pot1 show that all of these telomere-associated proteins use OB-folds to contact ssDNA. The relevance of OB-folds in telomere homeostasis has become even more evident in recent studies demonstrating OB-folds in human TPP1 and sequences in Stn1 that are similar to the OB-fold in RPA32 (14, 15, 21).

A search for novel OB-fold-containing proteins in fission yeast uncovered an Stn1-like protein, and this result led to the discovery of a Ten1-like protein. Our studies indicate that Stn1 and Ten1 are members of rapidly evolving protein families that are functionally conserved between *S. cerevisiae* and *S. pombe*. Stn1 and Ten1 are essential for telomere maintenance in fission yeast, they localize at telomeres, and their telomeric localization (as well as that of Pot1) correlates with the presence of telomeric ssDNA overhangs. The discovery of Stn1 and Ten1 orthologs supports the notion that Cdc13 and Pot1 are rapidly diverging orthologs (10). Stn1 appears to be the most conserved member of this group. Indeed, in addition to fungi, putative Stn1 orthologs are found in the sequenced genomes of primates, rodents, birds, amphibians, bony fishes, echinoderms, and plants. All of these organisms have Pot1 homologs. The exceptions are noteworthy. An Stn1 homolog is not detected in the sequenced genome of *Drosophila melanogaster*, a fact consistent with the absence of a Pot1 homolog and a mechanism of telomere maintenance that involves transposable elements instead of telomerase (33). These findings reinforce the idea that yeast species, including *S. cerevisiae*, are highly relevant experimental models for eukaryotic chromosome biology. However, we have not been able to detect Ten1-like proteins in species other than fungi. It is possible that Ten1 has been lost from other organisms, but we favor the idea that it has diverged beyond recognition by sequence-alignment tools.

It is particularly interesting that the alignments and secondary structure predictions of Stn1 homologs show that members of this conserved family of proteins have an OB-fold domain that is most similar to the OB-fold domain in RPA32, and the overall organizations of Stn1 and RPA32 are quite similar. In fact, the OB-fold domain of budding yeast Stn1 can be swapped into RPA32, rendering a protein that rescues *rpa32*Δ (21). It is also interesting that the fungal Ten1 homologs, which are only weakly similar at the primary sequence level, are also predicted to have an OB-fold domain. Both of these predictions need to be tested by determining these proteins' structures.

The existence of putative OB-folds in Stn1 and Ten1 provides additional support for the notion that Cdc13, Stn1, and Ten1 may form a trimeric complex that functions as a telomere-specific RPA complex (21). On this matter, it may be worth noting that the smaller subunits of RPA (RPA32 and RPA14) interact avidly, and it is thought that the formation of an RPA14–RPA32 heterodimer is a necessary precursor to the formation of the RPA complex (34). These relationships are interesting in light of our observation that Stn1 and Ten1 have a strong two-hybrid interaction.

However, we failed to detect yeast two-hybrid interactions between Pot1 and Stn1 or between Pot1 and Ten1, which is inconsistent with their forming an RPA-like complex. Our studies also indicate that there is a greater abundance of Pot1 at telomeres relative to Stn1 or Ten1. It is premature to speculate on the stoichiometric organization of the fission yeast telomere-capping complexes, but it is conceivable that *S. pombe* relies on two different telomere-capping complexes: a more abundant Pot1–Pot1 complex and a less abundant Stn1–Ten1 complex, both of which specifically interact with the 3′ ssDNA telomeric overhangs. Regardless of whether these proteins associate to form a telomere-specific RPA complex, it is clear that they are all required to shield chromosome ends from checkpoint and DNA repair proteins that would otherwise recognize the ends as double-strand breaks.

Finally, it is important to note the presence of a putative Stn1 homolog (OBFC1) in human cells, which suggests that the mechanism involved in telomere end protection is, in fact, more conserved than initially thought among yeast and humans. Further studies need to confirm whether OBFC1 is the functional homolog of the budding and fission yeast Stn1 proteins. The conserved yeast two-hybrid interactions of Stn1 and Ten1 suggest an obvious strategy for using human OBFC1 to find the human Ten1-like protein.

Materials and Methods

Yeast Strains and General Methods. The fission yeast strains used in this study are listed in SI Table 1. Deletion mutations and epitope-tagged strains were constructed as previously described (35, 36). Cell cultures and crosses were performed at 32°C. Heterozygous

diploid strains were sporulated, and the resulting tetrads were dissected and germinated on yeast extract medium-supplemented (YES) plates. Genotypes of the resulting cells were then distinguished by growing them on YES plates supplemented with hygromycin B or kanamycin.

Microscopy. For Hoechst 33342 staining, cells of the *pot1*Δ, *ten1*Δ, and *stn1*Δ mutants coming from colonies of ≈2,000 cells were analyzed; fluorescent images of DNA stained with 5 mg/ml Hoechst 33342 were merged with bright-field images of the cells. Cells came from colonies formed after spores were incubated at 30°C for 3 days. For detection of GFP signals, cells were grown at 30°C in rich medium (YES). Exponentially growing cells from each culture were concentrated by centrifugation before microscopy. Cells containing one or more GFP foci were considered positive. Images of GFP-tagged strains were obtained by using a Nikon Eclipse E800 microscope (Melville, NY) equipped with a Photometrics Quantix charge-coupled device camera (Tucson, AZ). Images were acquired with IPlab Spectrum software (Signal Analytics, Vienna, VA). More than 200 cells were counted for each strain.

For colocalization experiments, images were obtained with a DeltaVision (American Dynamics, San Diego, CA) optical sectioning microscope model 283 equipped with a yellow fluorescent protein/CFP filter set and a Photometrics CH350L cooled charge-coupled device camera. Images were acquired with a ×60, 1.4 numerical aperture objective and a ×1.5 optivar. Eight *Z* sections at 0.5-μm intervals were photographed and projected into one image by using softWoRx software (Applied Precision, Issaquah, WA). Control cells that expressed only one of the two fusion proteins were used to confirm that there was no significant bleedthrough of the GFP and CFP signals in the filter sets.

Yeast Two-Hybrid Constructs. Clontech (Mountain View, CA) Gal4-based Matchmaker Two-Hybrid System 3 was used for the yeast two-hybrid assay, following the supplier's instructions. The coding regions of the indicated proteins were amplified by PCR, and the restriction sites were introduced at the beginning (NdeI or NcoI sites) and end (BamHI or XhoI) of the ORFs to allow their fusion to the GAL4 activation domain or DNA-binding domain of the PGADT7 and PGBKT7, respectively. All fusion constructs were sequenced. Oligonucleotide primers used in this study are available upon request. *S. cerevisiae* AH109 strain was used as reporter strain. Interactions were verified by plating on selective minimal medium plates (SC): The control plate SC-TL (minimal medium lacking tryptophan and leucine) was used to select for cotransformation of plasmids, and the SC-HTL (lacking histidine, tryptophan, and leucine) plate was used to identify positive interactions.

Southern Blots and PFGE. Southern blotting and PFGE were performed as described elsewhere (26). Genomic DNA for Southern blots was digested with EcoRI and subjected to electrophoresis on 2% agarose gels. Staining with ethidium bromide was used to confirm equal loading in each lane. The DNA was transferred to a nylon membrane and hybridized to a 785-bp TAS1 probe obtained after digestion of the pNSU70 vector (Sanger Center, Cambridge, U.K.) with ApaI and EcoRI.

ChIP Assays. ChIP was performed as described in ref. 37. Briefly, DNA protein cross-links were induced *in vivo* by incubation of 5×10^8 cells in 1% formaldehyde for 20 min at room temperature, followed by the addition of glycine (final concentration 125 mM) for 5 min at room temperature. Cells were washed two times with ice-cold Tris-buffered saline, and cell pellets were frozen. Frozen cell pellets were then resuspended in lysis buffer [50 mM Hepes-KOH (pH 7.5)/140 mM NaCl/1 mM EDTA/1% Triton X-100] supplemented with protease inhibitors [0.2 mM *p*-amidinophenyl-methanesulfonyl fluoride and a Roche (Indianapolis, IN) protease inhibitor mixture]. Broken cells were sonicated until chromatin DNA was sheared into 500- to 700-bp fragments. Cell lysate was clarified by 15-min maximum-speed centrifugation in an Eppendorf (Boulder, CO) 5415C microcentrifuge at 4°C. Immunoprecipitation was performed on the cleared lysate with anti-myc 910 antibody bound to magnetic sheep anti-mouse IgG beads (Dynabeads M-280; Dynal Biotech, Lake Success, NY). PCR primers used to amplify the telomeric DNA (primers BAM136 and BAM137) have been previously described (26). Oligonucleotides used to amplify *act1*$^+$ sequences are available upon request.

Sequence Alignments. Sequences were aligned in ClustalW (www.ebi.ac.uk/clustalw/). The resulting alignments were adjusted manually and formatted with the BOXSHADE 3.21 program (www.ch.embnet.org/software/BOX_form.html).

We thank Charly Chahwan and the P. Russell, C. H. McGowan, and M. N. Boddy laboratories for their comments and suggestions and Harri Lempiainen and Aswhin Bhat for advice on PFGE. This work was supported by National Institutes of Health Grants GM59447 and CA77325 (to P.R.).

1. de Lange T (2005) *Genes Dev* 19:2100–2110.
2. Cech TR (2004) *Cell* 116:273–279.
3. Garvik B, Carson M, Hartwell L (1995) *Mol Cell Biol* 15:6128–6138.
4. Lin JJ, Zakian VA (1996) *Proc Natl Acad Sci USA* 93:13760–13765.
5. Nugent CI, Hughes TR, Lue NF, Lundblad V (1996) *Science* 274:249–252.
6. Booth C, Griffith E, Brady G, Lydall D (2001) *Nucleic Acids Res* 29:4414–4422.
7. Baumann P, Cech TR (2001) *Science* 292:1171–1175.
8. Theobald DL, Mitton-Fry RM, Wuttke DS (2003) *Annu Rev Biophys Biomol Struct* 32:115–133.
9. Bochkarev A, Bochkareva E (2004) *Curr Opin Struct Biol* 14:36–42.
10. Theobald DL, Cervantes RB, Lundblad V, Wuttke DS (2003) *Structure (London)* 11:1049–1050.
11. Mitton-Fry RM, Anderson EM, Hughes TR, Lundblad V, Wuttke DS (2002) *Science* 296:145–147.
12. Lei M, Podell ER, Cech TR (2004) *Nat Struct Mol Biol* 11:1223–1229.
13. Lei M, Podell ER, Baumann P, Cech TR (2003) *Nature* 426:198–203.
14. Xin H, Liu D, Wan M, Safari A, Kim H, Sun W, O'Connor MS, Songyang Z (2007) *Nature* 445:559–562.
15. Wang F, Podell ER, Zaug AJ, Yang Y, Baciu P, Cech TR, Lei M (2007) *Nature* 445:506–510.
16. Theobald DL, Wuttke DS (2004) *Structure (London)* 12:1877–1879.
17. Petreaca RC, Chiu HC, Eckelhoefer HA, Chuang C, Xu L, Nugent CI (2006) *Nat Cell Biol* 8:748–755.
18. Pennock E, Buckley K, Lundblad V (2001) *Cell* 104:387–396.
19. Grandin N, Damon C, Charbonneau M (2001) *EMBO J* 20:1173–1183.
20. Grandin N, Reed SI, Charbonneau M (1997) *Genes Dev* 11:512–527.
21. Gao H, Cervantes RB, Mandell EK, Otero JH, Lundblad V (2007) *Nat Struct Mol Biol* 14:208–214.
22. Kelley LA, MacCallum RM, Sternberg MJ (2000) *J Mol Biol* 299:499–520.
23. Bochkareva E, Korolev S, Lees-Miller SP, Bochkarev A (2002) *EMBO J* 21:1855–1863.
24. Altschul SF, Madden TL, Schaffer AA, Zhang J, Zhang Z, Miller W, Lipman DJ (1997) *Nucleic Acids Res* 25:3389–3402.
25. Schaffer AA, Aravind L, Madden TL, Shavirin S, Spouge JL, Wolf YI, Koonin EV, Altschul SF (2001) *Nucleic Acids Res* 29:2994–3005.
26. Nakamura TM, Moser BA, Russell P (2002) *Genetics* 161:1437–1452.
27. Fang G, Cech TR (1993) *Proc Natl Acad Sci USA* 90:6056–6060.
28. Taggart AK, Teng SC, Zakian VA (2002) *Science* 297:1023–1026.
29. Cooper JP, Nimmo ER, Allshire RC, Cech TR (1997) *Nature* 385:744–747.
30. Tomita K, Matsuura A, Caspari T, Carr AM, Akamatsu Y, Iwasaki H, Mizuno K, Ohta K, Uritani M, Ushimaru T, *et al.* (2003) *Mol Cell Biol* 23:5186–5197.
31. Ferreira MG, Cooper JP (2004) *Genes Dev* 18:2249–2254.
32. Loayza D, De Lange T (2003) *Nature* 423:1013–1018.
33. Pardue ML, Rashkova S, Casacuberta E, DeBaryshe PG, George JA, Traverse KL (2005) *Chromosome Res* 13:443–453.
34. Wold MS (1997) *Annu Rev Biochem* 66:61–92.
35. Bahler J, Wu JQ, Longtine MS, Shah NG, McKenzie A, III, Steever AB, Wach A, Philippsen P, Pringle JR (1998) *Yeast* 14:943–951.
36. Sato M, Dhut S, Toda T (2005) *Yeast* 22:583–591.
37. Noguchi E, Noguchi C, McDonald WH, Yates JR, III, Russell P (2004) *Mol Cell Biol* 24:8342–8355.